

THE INTERSTELLAR CLOUDS TOWARD 3C 154 AND 3C 353

S. R. FEDERMAN,^{1,2} NEAL J. EVANS II,² R. F. WILLSON,³ E. FALGARONE,⁴
 F. COMBES,⁴ AND B. M. SCHEUFELE³

Received 1987 January 30; accepted 1987 May 15

ABSTRACT

Molecular observations of the interstellar clouds toward the radio sources 3C 154 and 3C 353 were obtained in order to elucidate the physical conditions within the clouds. Maps of ^{12}CO emission in the $J = 1 \rightarrow 0$ and $J = 2 \rightarrow 1$ lines were compared with observations of the ^{13}CO , CH, and OH molecules. The peak emission in the ^{12}CO transitions *does not* occur in the direction of the continuum sources, and thus, an incomplete picture arises when only one line of sight in the two clouds is analyzed.

The cloud toward 3C 154 appears to have a low extinction, but a relatively high CO abundance, suggesting that it is similar to high-latitude clouds and CO-rich diffuse clouds. The cloud toward 3C 353 is considerably denser than that toward 3C 154 and may be more like a dark cloud.

Subject headings: interstellar: abundances — interstellar: molecules

I. INTRODUCTION

Many molecular observations have been made along the lines of sight toward extragalactic radio sources. Studies of molecular absorption or emission include the work on OH by Nguyen-Q-Rieu *et al.* (1976), Kazes, Crovisier, and Aubry (1977), and Crovisier, Kazes, and Brillet (1984), on CO by Combes *et al.* (1980) and Kazes and Crovisier (1981), and on H_2CO by Colgan, Salpeter, and Terzian (1986). Crovisier *et al.* measured emission from ^{13}CO in the directions of the radio continuum sources studied by Kazes and Crovisier (1981). The data for the clouds toward 3C 154 and 3C 353 indicate that the ratio of antenna temperatures $T_A^*(^{12}\text{CO})/T_A^*(^{13}\text{CO})$ for the $J = 1 \rightarrow 0$ transition is greater than 10. This value is significantly larger than the value found for dark clouds (cf. Dickman 1978), but is smaller than the lower limit deduced by Crutcher and Watson (1981) for the diffuse cloud toward the bright star ζ Ophiuchi. The ratio, however, is similar to that observed for high-latitude clouds (Magnani, Blitz, and Mundy 1985). The clouds toward 3C 154 and 3C 353, as well as the high-latitude clouds, appear to have properties intermediate between those of dark clouds and diffuse clouds.

Clouds with intermediate characteristics are of interest for several reasons. The chemistry of neutral molecules in diffuse clouds can be understood in terms of production through ion-molecule reactions and of destruction primarily through photoprocesses under steady state conditions (cf. van Dishoeck and Black 1986; Federman 1987). Similarly, the chemical models of dark clouds can reproduce many of the molecular observations when ion-molecule reactions, which occur under steady state conditions (cf. Prasad and Huntress 1980; Millar and Freeman 1984*a, b*), are considered. Several problems persist, such as the abundance of neutral carbon, suggesting that time-dependent evolution is necessary for a more complete picture of dark cloud chemistry (cf. Leung, Herbst, and Heubner 1985; Tarafdar *et al.* 1985). Clouds of intermediate density can be used to constrain the chemical models for both

diffuse clouds and dark clouds so that a single model is obtained to study the molecular chemistry of all interstellar clouds. To date the high-latitude clouds have been observed only in transitions of CO because of the lack of strong continuum sources in their directions. In order to accomplish the above goal, clouds of intermediate type must be identified and studied in detail.

The present work provides a detailed observational study of intermediate-type clouds. The clouds toward 3C 154 and 3C 353 were mapped in the $J = 2 \rightarrow 1$ and $J = 1 \rightarrow 0$ transitions of ^{12}CO , hereafter referred to CO. Additional observations of ^{13}CO in both transitions, of CH at 9 cm, and of OH at 18 cm, including maps in the lines of CH and OH, were obtained in order to determine the physical conditions appropriate for clouds of intermediate type. The observations are presented in § II, and the data are analyzed in § III. The final section (§ IV) includes the discussion and concluding remarks.

II. OBSERVATIONS

a) Carbon Monoxide

The emission from CO and ^{13}CO was measured with the 5 m telescope of the Millimeter Wave Observatory⁵ near Fort Davis, Texas. The measurements, made during several observing sessions between 1981 April and 1984 March, included the $J = 1 \rightarrow 0$ lines and the $J = 2 \rightarrow 1$ lines of CO and ^{13}CO . The beam size was 2/3 for the $J = 1 \rightarrow 0$ transitions and was 1/2 for the $J = 2 \rightarrow 1$ lines. The forward spillover and scattering efficiency (η_{fs}) was 0.83 for all the lines (see Kutner and Ulich 1981 for definitions of η_{fs}). The receivers used for most of the observations were cooled Schottky diode receivers. Most of the observations were acquired with 128 channel filter banks of 62.5 kHz and 250 kHz filters. Only the filter bank of 250 kHz filters was used in some of the earliest observations (1981 April). The data for 3C 353 of the $J = 2 \rightarrow 1$ line of CO taken in 1981 April were frequency-switched; the remaining data were taken by position-switching 15' W of 3C 154 [(0, 0): R.A. (1950) = $6^{\text{h}}10^{\text{m}}44^{\text{s}}.3$; decl. (1950) = $+26^{\circ}05'42''$] and

¹ Jet Propulsion Laboratory, California Institute of Technology.

² Department of Astronomy and Electrical Engineering Research Laboratory, University of Texas at Austin.

³ Department of Physics and Astronomy, Tufts University.

⁴ Departement de Radioastronomie, Observatoire de Meudon.

⁵ The Millimeter Wave Observatory is operated by the Electrical Engineering Research Laboratory of the University of Texas at Austin, with support from the National Science Foundation and McDonald Observatory.

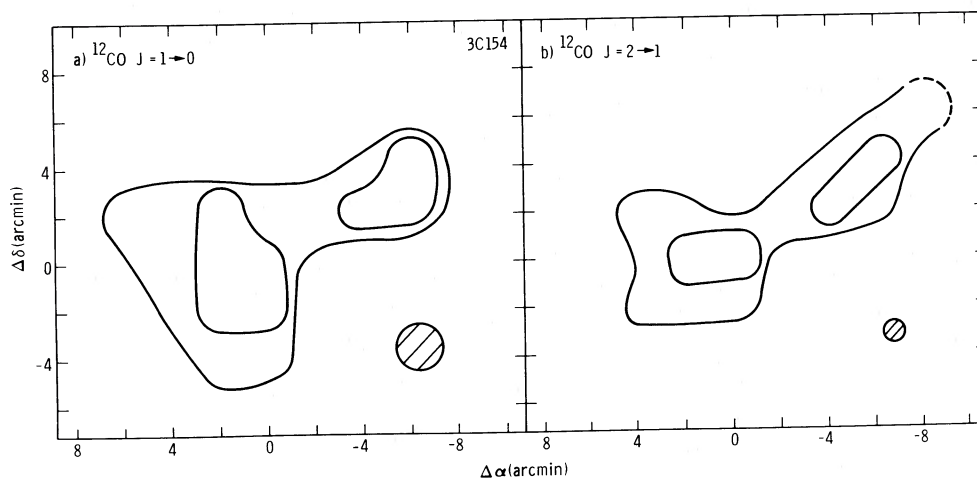


FIG. 1.—Contour maps of the ^{12}CO emission for the cloud toward 3C 154. (a) $T_A^*(J=1\rightarrow 0)$ from 2 K in 1 K increments. (b) $T_A^*(J=2\rightarrow 1)$ from 1 K in 0.8 K steps. The beam sizes are indicated in the lower right hand corners. The data for $J=2\rightarrow 1$ were taken at the positions observed for $J=1\rightarrow 0$. The (0, 0) corresponds to R.A. (1950) = $6^{\text{h}}10^{\text{m}}44^{\text{s}}.3$; decl. (1950) = $+26^{\circ}05'42''$.

15'S of 3C 353 [(0, 0): R.A. (1950) = $17^{\text{h}}17^{\text{m}}55^{\text{s}}.6$; decl. (1950) = $-00^{\circ}55'53''$].

The two clouds were mapped in both transitions of CO; the ^{13}CO lines were too weak to produce maps. Typical rms noise in the spectra from the 62.5 kHz filters (peak-to-peak noise/4) for the $J=1\rightarrow 0$ observations of CO was 0.5 K, while the rms noise for the CO $J=2\rightarrow 1$ lines was 0.25 K. The data were acquired with 2' spacings between adjacent points. Reference positions within the clouds, usually the (0, 0) position, were observed periodically to ensure consistency in the maps. The contour maps of T_A^* (the antenna temperature corrected for atmospheric effects) for the two CO lines for 3C 154 are shown in Figures 1a and 1b; the corresponding maps for 3C 353 are presented in Figures 2a and 2b. A finer grid (1' spacing) was obtained in the $J=2\rightarrow 1$ line around the peak emission so that variations of the line parameters could be studied at higher spatial resolution; no significant variations were noticed. Additional evidence that the structure is resolved is

that ^{13}CO data of the $J=1\rightarrow 0$ line taken with the 2.5 m telescope at Bordeaux (Baudry *et al.* 1980) did not differ from the data taken at the Millimeter Wave Observatory. Table 1 displays T_A^* , the velocity of line center v_{LSR} , and the full width at half-maximum Δv for all the carbon monoxide data at the positions of the CO peak for the two clouds. The (0, 0) position for the cloud toward 3C 353 is also shown. Our measurements agree with previous observations of carbon monoxide (Combes *et al.* 1980; Crovisier *et al.*).

b) CH and OH

The observations of the $F=1-1$ $^2\Pi_{1/2}$ $J=1/2$ Λ doublet transition of CH at 9 cm were made in 1984 June using the 43 m telescope of the National Radio Astronomy Observatory.⁶ The $F=1-1$ and $F=2-2$ transitions of the $^2\Pi_{3/2}$ $J=3/2$

⁶ The National Radio Astronomy Observatory is operated by the Associated Universities, Inc. under contract with the National Science Foundation.

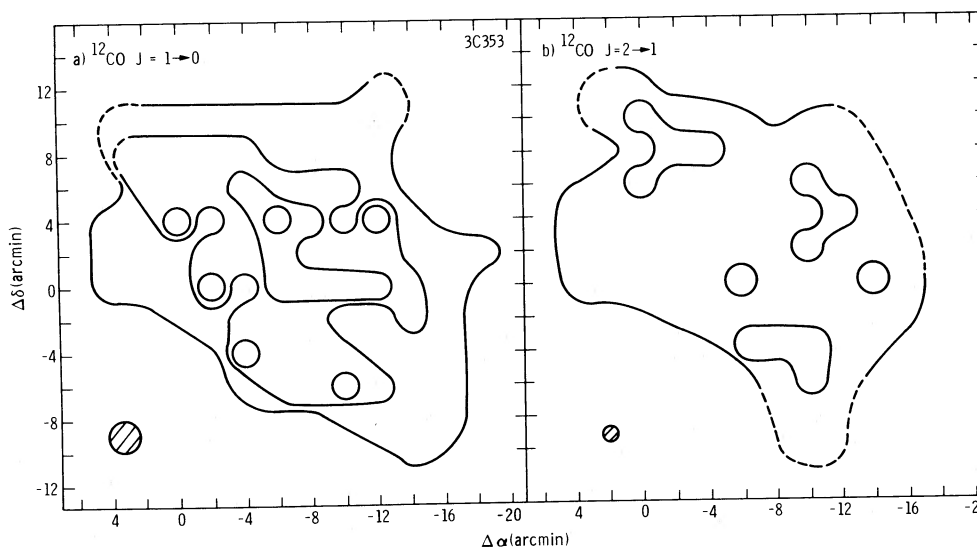


FIG. 2.—Contour maps of the ^{12}CO emission from the cloud toward 3C 353. (a) $T_A^*(J=1\rightarrow 0)$ from 2 K in steps of 1 K. (b) $T_A^*(J=2\rightarrow 1)$ from 1 K with 1 K contours. Beam sizes are shown in the lower left hand corners. Map of $J=2\rightarrow 1$ emission sampled as in Fig. 1. The (0, 0) position is R.A. (1950) = $17^{\text{h}}17^{\text{m}}55^{\text{s}}.6$ and decl. (1950) = $-00^{\circ}55'53''$.

TABLE 1
 CARBON MONOXIDE RESULTS

POSITION	$J = 1 \rightarrow 0$			$J = 2 \rightarrow 1$		
	T_A^* (K)	v_{LSR} (km s ⁻¹)	Δv (km s ⁻¹)	T_A^* (K)	v_{LSR} (km s ⁻¹)	Δv (km s ⁻¹)
3C 154						
(0, 0)	3.2 ^a	-2.1	1.9	2.0	-2.0	1.4
	0.34 ^a	-2.1	1.7	<0.15
3C 353						
(0, 0)	2.7	+0.1	0.6	1.5	-0.1	~0.8
				<0.3
(-10, 0)	4.8	-0.2	0.7	1.8	-0.1	~0.9
	0.53 ± 0.08	-0.0	0.4	0.57 ± 0.15	+0.2	0.7

^a Top line refers to ¹²CO data, and bottom line refers to ¹³CO data.

doublet line of OH at 18 cm were measured with the same telescope in 1984 February. The half-power beamwidths are 9' and 18' for CH and OH. Maps were made with half-beam spacings of 4.5 and 10' for CH and OH. The setups for the autocorrelators are described by Federman and Willson (1984). The spectra, which were acquired by frequency-switching, have an effective resolution of ~0.40 km s⁻¹. All detections were fitted by a least-squares iterative procedure with a Gaussian function to obtain the line temperature T_L , v_{LSR} , and Δv . The results of the fitting procedure are displayed in Table 2 for CH and Table 3 for OH. The upper limits for the line temperatures are twice the rms noise in the spectra.

For 3C 154, OH absorption was seen but no lines of CH were detected. For 3C 353 OH absorption/emission and CH emission were mapped over a large portion of the cloud extent, as defined by the 2 K level of the emission from the $J = 1 \rightarrow 0$ transition of CO. Figures 3 and 4 present the maps for the CH lines and the OH lines, respectively; the numbers correspond to T_L with a minus sign indicating absorption. In Figure 4, the

line temperature of the 1.667 GHz line is shown above that for the 1.665 GHz line.

III. RESULTS

a) 3C 154

The contour maps of CO emission in the $J = 1 \rightarrow 0$ and $J = 2 \rightarrow 1$ transitions are similar with peaks in T_A^* of 3–5 K in the $J = 1 \rightarrow 0$ line and of ~2 K in the $J = 2 \rightarrow 1$ line. Over the surface of the cloud, the ratio $T_A^*(2 \rightarrow 1)/T_A^*(1 \rightarrow 0)$ is nearly constant at 0.5 ± 0.1 . Within the precision of the observations, v_{LSR} and Δv are constant across the cloud with respective values of -1.9 km s⁻¹ and 1.5 km s⁻¹. At the (0, 0) position, where $T_A^*(1 \rightarrow 0)$ is 3.2 K, the antenna temperature for the same ¹³CO line is 0.34 ± 0.04 K, confirming the ratio of antenna temperature between CO and ¹³CO of 10 that was determined by Crovisier *et al.* The ratio of the $J = 2 \rightarrow 1$ lines is even higher (> 13). These ratios for the two isotopic species are intermediate between the ratios (3–5) for dark clouds (cf.

 TABLE 2
 CH DATA

Position	T_L (K)	v_{LSR} (km s ⁻¹)	Δv (km s ⁻¹)	$N(\text{CH})$ (cm ⁻²)	A_v (mag)
3C 154					
(0, 0)	<0.017	...	(1.5) ^a	<2.0(13) ^b	<1.1
(-4.5, 0)	<0.021	...	(1.5)	<2.5(13)	<1.2
(+4.5, 0)	<0.014	...	(1.5)	<1.7(13)	<0.9
(0, +4.5)	<0.012	...	(1.5)	<1.5(13)	<0.8
(0, -4.5)	<0.013	...	(1.5)	<1.6(13)	<0.8
(-10, 0)	<0.013	...	(1.5)	<1.6(13)	<0.8
3C 353					
(-10, 0)	0.053 ± 0.006	-0.38 ± 0.16	3.11 ± 0.40	1.1(14)	5.5
(-14.5, 0)	0.047 ± 0.005	-0.17 ± 0.09	1.76 ± 0.23	5.6(13)	2.8
(-5.5, 0)	0.049 ± 0.008	-0.17 ± 0.06	1.05 ± 0.14	3.5(13)	1.8
(-10, +4.5)	0.078 ± 0.009	+0.07 ± 0.13	2.20 ± 0.32	1.2(14)	6.0
(-10, -4.5)	0.048 ± 0.006	-0.31 ± 0.10	1.71 ± 0.24	5.5(13)	2.8
(-20, 0)	<0.010	...	(2.0) ^c	<1.3(13)	<0.7
(-5.5, +4.5)	0.042 ± 0.006	-0.22 ± 0.15	2.16 ± 0.36	6.1(13)	3.1
(-14.5, +4.5)	0.052 ± 0.006	-0.30 ± 0.08	1.44 ± 0.20	5.0(13)	2.5
(-5.5, -4.5)	0.062 ± 0.008	+0.03 ± 0.09	1.31 ± 0.21	5.5(13)	2.8

^a 1.5 km s⁻¹ estimated from CO data.

^b 1.3(13) = 1.3×10^{13} .

^c 2.0 km s⁻¹ estimated from other CH data.

TABLE 3
OH DATA

Position	T_L (K)	v_{LSR} (km s ⁻¹)	Δv (km s ⁻¹)	T_c (K)	$N(\text{OH})^a$ (cm ⁻²)	A_V (mag)
3C 154						
(0, 0)	-0.041 ± 0.009 ^b	-2.34 ± 0.07	0.59 ± 0.16	1.2	2.9(13)	0.4
	<0.024 ^b			
(-10, 0)	<0.022
	... ^c	... ^c	... ^c			
3C 353						
(0, 0)	-1.14 ± 0.06	+0.10 ± 0.02	0.58 ± 0.04	15.3	3.3(13)	0.4
	-0.48 ± 0.04	+0.17 ± 0.02	0.65 ± 0.06			
(-10, 0)	-0.42 ± 0.03	+0.13 ± 0.02	0.60 ± 0.05	8.2	2.6(13)	0.3
	-0.27 ± 0.02	+0.18 ± 0.02	0.56 ± 0.05			
(-20, 0)	+0.027 ± 0.002	-0.20 ± 0.13	3.14 ± 0.31	...	3.2(14)	4.0
	+0.016 ± 0.001	+0.21 ± 0.14	4.42 ± 0.34			
(-10, -10)	-0.15 ± 0.01	+0.08 ± 0.02	0.45 ± 0.04	2.7	2.3(13)	0.3
	... ^c	... ^c	... ^c			
(-10, +10)	-0.16 ± 0.01	+0.12 ± 0.02	0.51 ± 0.05	1.9	3.6(13)	0.5
	... ^c	... ^c	... ^c			

^a For absorption lines, $N(\text{OH})$ was derived from the 1.667 GHz data.
^b For each position, the upper line corresponds to the 1.667 GHz data, while the lower line is the 1.665 GHz data.
^c No 1.665 GHz data were taken.

Dickman 1978) and those of diffuse clouds (Crutcher and Watson 1981), where the ratio approaches the terrestrial value.

The physical conditions within the cloud can be estimated from the carbon monoxide emission. The ratios of CO to ¹³CO emission discussed above indicate that the CO emission is optically thick. The excitation temperatures derived under this assumption are 7.1 K ($J = 1 \rightarrow 0$ line) and 6.7 K ($J = 2 \rightarrow 1$ line); the similarity is consistent with the thermalization of the CO lines and leads to the conclusion that the cloud kinetic

temperature (T_K) is ~ 7 K. If the ¹³CO were also thermalized, we should be able to use the LTE method for deriving the ¹³CO column density (N_{13}) and the results for the two lines would agree. Instead we find $N_{13}(\text{LTE}) = 6.5 \times 10^{14}$ cm⁻² from the $J = 1 \rightarrow 0$ line and $N_{13}(\text{LTE}) < 3.0 \times 10^{14}$ cm⁻² from the $J = 2 \rightarrow 1$ line. The substantial discrepancy between these estimates indicates that the excitation temperature must in fact drop rapidly with J . In this case the ($J = 2 \rightarrow 1$)/($J = 1 \rightarrow 0$) line ratio and the $J = 1 \rightarrow 0$ line strength may be

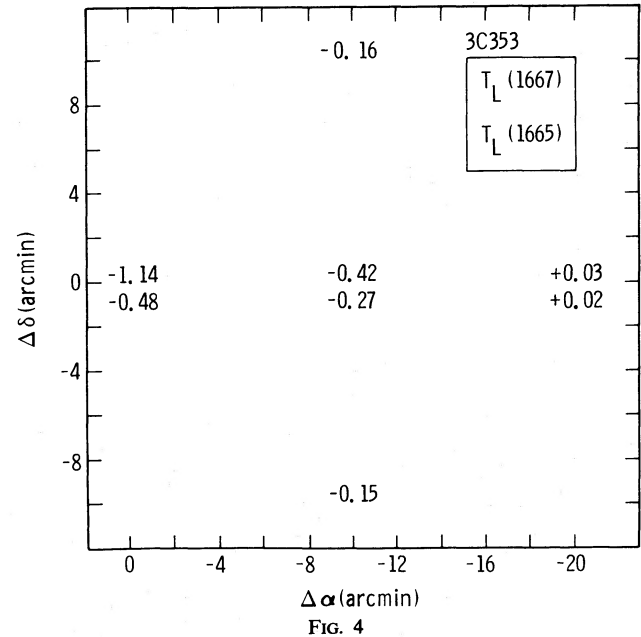
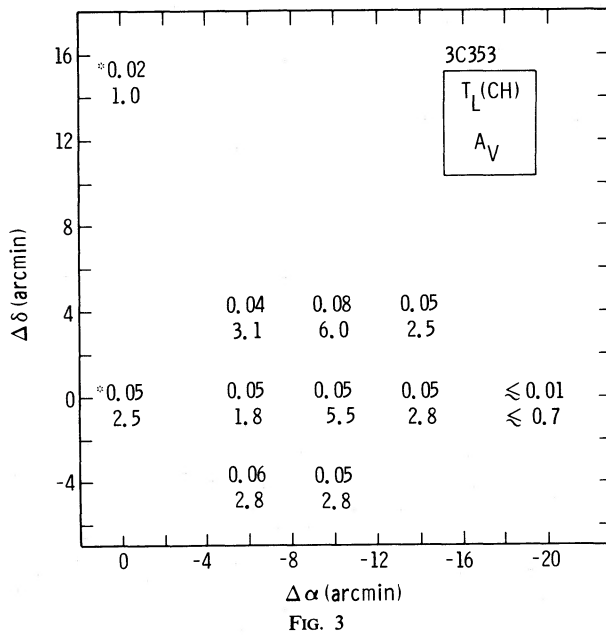


FIG. 3.—A graphical representation of the CH results for the cloud in the direction of 3C 353. The upper number is $T_L(\text{CH})$ (in K), and the lower number is the visual extinction A_V in mag deduced from $N(\text{CH})$ at the position. The beam size for the CH observations is 9'. Data from Hjalmarson *et al.* (1977) are indicated by asterisks.

FIG. 4.—The OH results for the cloud toward 3C 353. In K, $T_L(1667)$ is displayed above $T_L(1665)$. Where only one number appears, the data correspond to the 1667 MHz line. Negative values represent absorption. The beam size is 18' for the OH observations.

used to set an upper limit on the density of the cloud. Using the Large Velocity Gradient (LVG) model of Goldsmith, Young, and Langer (1983) for $T_K = 10$ K, we obtain a density (n) less than $1.6 \times 10^3 \text{ cm}^{-3}$. This limit allows us to constrain the fraction of the population in the $J = 1$ state to $0.3 \leq F_1 \leq 0.5$, leading to $5 \times 10^{14} \text{ cm}^{-2} \leq N_{13} \leq 9 \times 10^{14} \text{ cm}^{-2}$, with the lower end of the range being more likely.

The column density of CH can be obtained from the expression given by Rydbeck *et al.* (1976) with a microwave background temperature of 2.8 K and a beam efficiency of 0.6. The upper limits for $N(\text{CH})$ shown in Table 2 include the assumptions that the CH is not clumped on scales smaller than the telescope beam, that $T_{\text{ex}}(\text{CH})$ is 7 K, the approximate kinetic temperature of the gas, and that the velocity width is 1.5 km s^{-1} . $N(\text{CH})$ may exceed our upper limits if the cloud does not fill the telescope beam (note the small extent of the 2 K contour of the CO $J = 1 \rightarrow 0$ line).

In addition to constraining $N(\text{CH})$, the data for CH are useful in deriving an upper limit to the extinction through the cloud (cf. Federman and Willson 1984). The extinction is determined by applying well-founded relationships, applicable to both diffuse clouds and dark clouds, between molecular column densities $N(X)$ for species X and A_V . The use of the relationship, $N(\text{CH})/A_V = 2 \times 10^{13} \text{ cm}^{-2} \text{ mag}^{-1}$ (Sandell *et al.* 1981; Federman 1982), indicates that the extinction through the cloud toward 3C 154 is less than about 1 mag.

Toward 3C 154 OH is seen in absorption. For absorption lines $N(\text{OH})$ is determined according to the procedure described by Dickey, Crovisier, and Kazes (1981). The results for 3C 154 lead to a value of $2.9 \times 10^{13} \text{ cm}^{-2}$ for $N(\text{OH})$ at the (0, 0) position when a continuum temperature of 1.2 K, an upper limit for T_L , the off-source line temperature, of 0.022 K, and a cloud filling factor of 0.5 are used. The excitation temperature and optical depth are found to be 4.2 K and 0.053, respectively. The expression derived by Crutcher (1979) for estimating the extinction from $N(\text{OH})$, $N(\text{OH})/A_V = 8 \times 10^{13} \text{ cm}^{-2} \text{ mag}^{-1}$, yields 0.4 mag of extinction through the cloud, a value slightly less than the one deduced from the upper limit for CH emission. Similar results for OH were obtained by Nguyen-Q-Rieu *et al.* (1976), Kazes *et al.*, Dickey *et al.*, and Crovisier *et al.*

The velocity for OH absorption and the width of the OH line differ from the corresponding line parameters for CO emission. While the difference in the velocity of the lines ($\sim 0.3 \text{ km s}^{-1}$) probably is within the uncertainties for the deduced line parameters, the width of the OH line is only 0.6 km s^{-1} , compared to $\sim 1.5 \text{ km s}^{-1}$ for the CO lines. These differences are also present in the previous measurements of OH and CO (Crovisier *et al.*). The difference in velocity widths between the two molecular lines probably arises because absorption-line measurements sample a narrow beam through the cloud while emission-line measurements sample the systematic velocity dispersion over a larger area in the cloud. Saturation of the CO lines probably does not cause the observed difference in linewidth for the cloud toward 3C 154 since the linewidth of ^{13}CO is not much less than that for CO.

The low extinction through the cloud toward 3C 154, based on the CH upper limit and the OH measurement, suggest that this is a diffuse cloud, similar to the cloud toward ζ Oph. However, the CO data indicate that the cloud toward 3C 154 is cooler ($T_K = 7$ K) than the ζ Oph cloud ($T_K = 40$ K) and the ^{13}CO data indicate much larger CO abundances. If the isotopic ratio is terrestrial, the implied CO column density is

$4\text{--}8 \times 10^{16} \text{ cm}^{-2}$, similar to that found in high-latitude clouds (Magnani, Blitz, and Mundy 1985) and the CO-rich diffuse clouds (Lada and Blitz 1987). If the A_V (0.4 mag) estimated from the OH data applies to the region of ^{13}CO emission and if we take $N(\text{H}_2) = 9.4 \times 10^{20} \text{ cm}^{-2} A_V$, we find that $x(\text{CO})$, the abundance of CO, equals $1\text{--}2 \times 10^{-4}$, which would be comparable to or larger than that inferred for dark clouds. The abundances for CH and OH in the 3C 154 cloud are slightly larger than the corresponding ones in the ζ Oph cloud, but less than those in dark clouds.

b) 3C 353

Mapping of this cloud in CO reveals that the line of sight to the continuum source is at the edge of the cloud. The center of the cloud is approximately $8'\text{--}10'$ west of the position of the source.

Unlike the situation in 3C 154, the contour maps of CO emission toward 3C 353 in the two rotational transitions are quite different. The $J = 1 \rightarrow 0$ line is strongest near the center of the cloud; the emission from the $J = 2 \rightarrow 1$ is very weak there, with $T_A^*(J = 2 \rightarrow 1)/T_A^*(J = 1 \rightarrow 0) < 0.4$ at $(-10, 0)$. In the outer regions of the cloud, however, the ratio of antenna temperatures for the two lines is approximately constant at a value of 0.5. Large optical depths in the $J = 2\text{--}1$ transition toward the center of the cloud and a low kinetic temperature are the probable causes for the difference in contour maps. Evidence for large optical depths includes the fact that the widths of the ^{13}CO lines are significantly less than the corresponding lines of CO. A possible consequence of self-absorption, velocity shifts between lines from different isotopic species of carbon monoxide, may also be discernible in our data. The results presented in Table 1 indicate a systematic shift of $\sim 0.2\text{--}0.3 \text{ km s}^{-1}$. However, the profile of the $J = 2 \rightarrow 1$ transition does not show any deviation from a single Gaussian, as can arise from self-absorption.

Another difference between the carbon monoxide maps for the two clouds is that in the cloud toward 3C 353 there is an apparent velocity gradient in the NW to SE direction. Figure 5 illustrates the gradient by showing lines of constant v_{LSR} superposed on the 2 K contour of the $J = 1 \rightarrow 0$ map. Both lines of CO indicate a velocity gradient; the more extensive map in $J = 1 \rightarrow 0$ presents a better representation of the gradient. The data from the CH and OH measurements displayed in Tables 2 and 3, although of poorer spatial and velocity resolution, are consistent with results from CO. Comparison with previously published data is limited because most of the data were obtained only toward the extragalactic radio source.

A comparison of the emission lines from the different molecular species reveals an interesting trend. There is a correlation between beam size and velocity width, namely $\Delta v_{\text{em}}(\text{OH}) > \Delta v(\text{CH}) > \Delta v(\text{CO}) \approx \Delta v_{\text{ab}}(\text{OH})$, where em and ab stand for emission and absorption. The presence of the velocity gradient seen in the CO data will cause the widths of the molecular lines observed with large beams to be larger.

We have detections in both the $J = 1 \rightarrow 0$ and $J = 2 \rightarrow 1$ lines of CO and ^{13}CO at the $(-10, 0)$ position, which is actually near the center of the cloud, and an analysis similar to that done for the 3C 154 cloud is possible. In the 3C 353 cloud, however, the excitation temperatures of the two CO lines do not agree very well; $T_{\text{ex}} = 9.1$ K is obtained from the $J = 1 \rightarrow 0$ line and $T_{\text{ex}} = 6.4$ K is derived from the $J = 2 \rightarrow 1$ line. While this discrepancy could be interpreted as a failure to thermalize the CO levels, the ^{13}CO analysis described below indicates

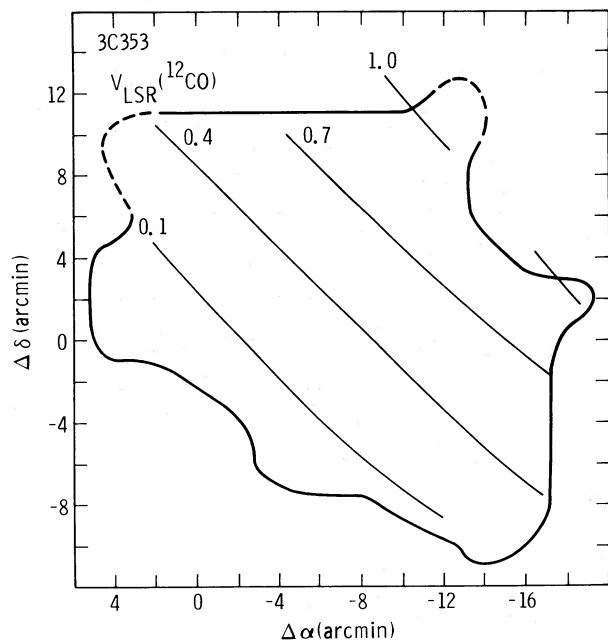


FIG. 5.—The velocity field for the 3C 353 cloud. The thin lines indicate v_{LSR} in units of km s^{-1} . The thicker curve represents the 2 K contour of the $J = 1 \rightarrow 0$ emission from ^{12}CO , as in Fig. 2a.

densities high enough for thermalization. We instead take 9 K to be the kinetic temperature and attribute the weakness of the $J = 2 \rightarrow 1$ line to self-absorption, as discussed above. The ^{13}CO column density derived from the LTE analyses is $N_{13}(\text{LTE}) = 2.4 \times 10^{14} \text{ cm}^{-2}$ ($J = 1 \rightarrow 0$) and $5.8 \times 10^{14} \text{ cm}^{-2}$ ($J = 2 \rightarrow 1$). Note that the discrepancy between the two estimates is in the opposite direction from that found in the cloud toward 3C 154, reflecting the much higher ($J = 2 \rightarrow 1$)/($J = 1 \rightarrow 0$) line ratio for ^{13}CO seen in 3C 353 ($-10, 0$). This high ratio also results in a much higher density estimate ($n = 1.6 \times 10^4 \text{ cm}^{-3}$) and lower abundance estimate [$x(^{13}\text{CO}) = 7.0 \times 10^{-9}$] from the LVG models at 10 K (Goldsmith *et al.*). The abundance estimate is almost surely too low and suggests the presence of inhomogeneities within the beam and/or optical depth effects in the ^{13}CO lines. The fractional abundances in the $J = 1$ and $J = 2$ states for these physical conditions are $f_1 = 0.45$ and $f_2 = 0.23$, yielding estimates for N_{13} of $2.2 \times 10^{14} \text{ cm}^{-2}$ and $3.4 \times 10^{14} \text{ cm}^{-2}$, in reasonable internal agreement, and in agreement with $N_{13}(\text{LTE})$ from the $J = 1 \rightarrow 0$ line, but about half the value derived from the $J = 2 \rightarrow 1$ line. Thus, this position in 3C 353 has ^{13}CO column densities less than those in 3C 154, but a density an order of magnitude larger.

The hydroxyl radical, OH, is observed in absorption when the telescope beam includes the extragalactic source 3C 353 and in emission at a position far from the direction of the source. In order to calculate $N(\text{OH})$ from emission-line data, the excitation temperature of the OH lines and the optical depth in the lines are again required. These two parameters can be found with the assumption that $T_{\text{ex}}(1665) = T_{\text{ex}}(1667)$ and that $\tau_{1665} = 5/9\tau_{1667}$, where 1665 and 1667 are the frequencies in MHz of the main-line transitions of OH. An expression similar to the one discussed above for CH is then appropriate in calculating $N(\text{OH})$. The results presented in Table 3 for (0, 0) are very similar to the results of Nguyen-Q-Rieu *et al.* (1976).

The extinction implied toward $(-10, 0)$ is 0.3 mag. As with the data for 3C 154, the velocity width of the absorption lines is significantly less than the width of the emission lines; the measurements of emission lines sample a larger systematic dispersion in velocities because of the bigger beam.

The CH lines can be analyzed, in the same way as was done for the CH upper limits toward 3C 154, to obtain $N(\text{CH})$ and A_V . These are given in Table 2. The estimated A_V toward $(-10, 0)$ is 5.5 mag, much larger than is suggested by the OH absorption line. Part of this discrepancy is caused by the much greater linewidth of CH. If this line is mostly caused by unresolved systematic motions, then an overestimate of A_V will result. If the line width of ^{13}CO ($\sim 0.7 \text{ km s}^{-1}$) is used, the resulting A_V is 1.2 mag. This is still 4 times larger than the extinction estimated from OH. Anomalies in the excitation of the two OH lines (Crutcher 1979) may cause the remaining difference.

If the CO isotopic ratios are terrestrial, the CO column density toward $(-10, 0)$ is $2\text{--}3 \times 10^{16} \text{ cm}^{-2}$. If we take $A_V = 1\text{--}5$ mag, as suggested by CH, we get $x(\text{CO}) = 0.4\text{--}3.0 \times 10^{-5}$; if instead $A_V = 0.3$ mag, as suggested by OH, $x(\text{CO}) = 1.2\text{--}9.0 \times 10^{-5}$, comparable to dark clouds. Further progress on this cloud would require a better estimate of A_V .

IV. DISCUSSION

The analysis of these two clouds illustrates the utility of observations of the $J = 2 \rightarrow 1$ line of ^{13}CO . The data in Table 1 show that the two clouds look very similar in the $J = 1 \rightarrow 0$ CO and ^{13}CO emission, but that the $J = 2 \rightarrow 1$ emission characteristics are very different. While quantitative interpretation of these observations in terms of densities and abundances is quite uncertain, there is no doubt that the $(-10, 0)$ position in 3C 353 is much denser than the (0, 0) position in 3C 154. The CO abundances in these clouds appear to be quite high, suggesting that they are related to high-latitude clouds and CO-rich diffuse clouds. The main source of uncertainty in the present analysis is the extinction estimate; if $A_V \approx 5$ mag for 3C 353, it is more like a standard dark cloud.

The above derivation for the abundances of CO in the clouds toward 3C 154 and 3C 353 is appropriate when the emission from CO and ^{13}CO arises from the same parcel of gas. The cloud toward 3C 353 may be more like the clouds modeled by Falgarone and Puget (1985), where the ^{13}CO emission comes from cooler, denser regions closer to the center of the cloud than from where the CO emission arises. However, the low kinetic temperature derived from the CO lines and the moderately low extinction for this cloud probably indicate similar emitting regions for the two isotopic species.

Because these two clouds lie in front of continuum radio sources, additional measurements of other species can be performed to constrain further the deduced properties. Absorption of H_2CO at 6 cm has been reported for both clouds. Colgan *et al.* found an abundance for H_2CO relative to OH of 0.12 in the cloud toward 3C 154, and Nguyen-Q-Rieu *et al.* (1976) obtained an abundance ratio of ~ 0.04 for the cloud toward 3C 353. Considering the signal-to-noise ratio for the data toward 3C 154, the two results are consistent with a ratio $x(\text{H}_2\text{CO})$ to $x(\text{OH})$ of ~ 0.05 . When the results of the analysis from the present work are used to constrain chemical models, the lower value for the ratio of H_2CO to OH seems more appropriate for the clouds toward 3C 154 and 3C 353. In particular, chemical models of a cloud with an extinction of 1–2 mag, a density of $\sim 10^3\text{--}10^4 \text{ cm}^{-3}$, and $x(\text{CO}) \approx 10^{-5}$ –

10^{-4} yield $x(\text{H}_2\text{CO})/x(\text{OH})$ of ~ 0.01 (e.g., Mitchell, Ginsburg, and Kuntz 1978; Watt 1983). It must be stressed, however, that the line of sight toward a continuum source need not pass through the cloud core; the cloud in the direction of 3C 353 is a case in point.

The properties of the cloud toward 3C 154 are similar to those of high-latitude molecular clouds (Magnani, Blitz, and Mundy 1985), where the ratio of $T_A^*(\text{CO})$ to $T_A^*(^{13}\text{CO})$ is typically 10. The deduced extinction and the antenna temperatures for the carbon monoxide transitions are also similar. The cloud in front of 3C 154 has a smaller extent on the sky, however, than do typical high-latitude clouds. This result may indicate that the cloud toward 3C 154 is farther from the Sun than the high-latitude clouds, which are at an average distance of 100 pc from the Sun (Magnani, Lada, and Blitz 1986). The correspondence between the 3C 154 cloud and high-latitude CO clouds leads us to suggest that more can be learned about

high-latitude clouds through molecular observations of species like CH and OH. Since these molecules are also observed in emission, no background radio source is necessary for the measurements.

We appreciate the comments on an earlier version of the manuscript provided by Lee Mundy. Our discussions with Leo Blitz led to substantial improvements in the analysis. S. R. F. was supported in part by grant F-623 from the Robert A. Welch Foundation, while at the University of Texas, with an NAS/NRC Research Associateship at the Jet Propulsion Laboratory, and by the Jet Propulsion Laboratory, California Institute of Technology, under a contract with the National Aeronautics and Space Administration. Partial support for this work comes from National Science Foundation grants AST 81-16403, AST 83-12332, and AST 86-11784 to the University of Texas at Austin.

REFERENCES

- Baudry, A., et al. 1980, *J. Ap. Astr.*, **1**, 193.
 Colgan, S. W. J., Salpeter, E. E., and Terzian, Y. 1986, *A.J.*, **91**, 107.
 Combes, F., Falgarone, E., Guibert, J., and Nguyen-Q-Rieu. 1980, *Astr. Ap.*, **90**, 88.
 Crovisier, J., Kazes, I., and Brillet, J. 1984, *Astr. Ap.*, **138**, 237.
 Crutcher, R. M. 1979, *Ap. J.*, **234**, 881.
 Crutcher, R. M., and Watson, W. D. 1981, *Ap. J.*, **244**, 855.
 Dickey, J. M., Crovisier, J., and Kazes, I. 1981, *Astr. Ap.*, **98**, 271.
 Dickman, R. L. 1978, *Ap. J. Suppl.*, **37**, 407.
 Falgarone, E., and Puget, J. L. 1985, *Astr. Ap.*, **142**, 157.
 Federman, S. R. 1982, *Ap. J.*, **257**, 125.
 ———. 1987, in *IAU Symposium 120, Astrochemistry*, ed. M. S. Vardya and S. P. Tarafdar (Dordrecht:Reidel), p. 123.
 Federman, S. R., and Willson, R. F. 1984, *Ap. J.*, **283**, 626.
 Goldsmith, P. F., Young, J. S., and Langer, W. D. 1983, *Ap. J. Suppl.*, **51**, 203.
 Hjalmarson, A., et al. 1977, *Ap. J. Suppl.*, **35**, 263.
 Kazes, I., and Crovisier, J. 1981, *Astr. Ap.*, **101**, 401.
 Kazes, I., Crovisier, J., and Aubry, D. 1977, *Astr. Ap.*, **58**, 403.
 Kutner, M. L., and Ulich, B. L. 1981, *Ap. J.*, **250**, 341.
 Lada, E. A., and Blitz, L. 1987, in preparation.
 Leung, C. M., Herbst, E., and Huebner, W. F. 1985, *Ap. J. Suppl.*, **56**, 231.
 Magnani, L., Blitz, L., and Mundy, L. 1985, *Ap. J.*, **295**, 402.
 Magnani, L., Lada, E. A., and Blitz, L. 1986, *Ap. J.*, **301**, 395.
 Millar, T. J., and Freeman, A. 1984a, *M.N.R.A.S.*, **207**, 405.
 ———. 1984b, *M.N.R.A.S.*, **207**, 425.
 Mitchell, G. F., Ginsburg, J. L., and Kuntz, P. J. 1978, *Ap. J. Suppl.*, **38**, 39.
 Nguyen-Q-Rieu, Winnberg, A., Guibert, J., Lepine, J. R. D., Johansson, L. E. B., and Goss, W. M. 1976, *Astr. Ap.*, **46**, 413.
 Prasad, S. S., and Huntress, W. T. 1980, *Ap. J. Suppl.*, **43**, 1.
 Rydbeck, O. E. H., Kollberg, E., Hjalmarson, A., Sume, A., Ellder, J., and Irvine, W. M. 1976, *Ap. J. Suppl.*, **31**, 333.
 Sandell, G., Johansson, L. E. B., Nguyen-Q-Rieu, and Mattila, K. 1981, *Astr. Ap.*, **97**, 317.
 Tarafdar, S. P., Prasad, S. S., Huntress, W. T., Villere, K. R., and Black, D. C. 1985, *Ap. J.*, **289**, 220.
 van Dishoeck, E. F., and Black, J. H. 1986, *Ap. J. Suppl.*, **62**, 109.
 Wannier, P. G. 1980, *Ann. Rev. Astr. Ap.*, **18**, 399.
 Watt, G. D. 1983, *M.N.R.A.S.*, **205**, 321.

F. COMBES and F. FALGARONE: DEMIRM, Observatoire de Paris, 92195 Meudon Cedex, France

NEAL EVANS II: Department of Astronomy, University of Texas at Austin, Austin, TX 78712

S. R. FEDERMAN: M.S. 183-601, Jet Propulsion Laboratory, 4800 Oak Grove Drive, Pasadena, CA 91109

B. M. SCHEUFELE and R. F. WILLSON: Department of Physics and Astronomy, Tufts University, Medford, MA 02155